Journal of Applied Mathematics and Computational Mechanics 2019, 18(4), 85-94
www.amcm.pcz.pl p-ISSN 2299-9965
DOI: 10.17512/jamcm.2019.4.08 e-ISSN 2353-0588

THE CONTROL OF STABILITY OF A COLUMN SUBJECTED TO SPECIFIC LOAD

Krzysztof Sokół

Institute of Mechanics and Machine Design Foundation, Czestochowa University of Technology
Częstochowa, Poland
sokol@imipkm.pcz.pl

Received: 3 October 2019; Accepted: 18 December 2019

Abstract. In this paper the problem of vibration control of a multi-member column subjected to the specific load is investigated. The vibration control is realized with the use of the piezoceramic element in the form of a rod that is connected to the host structure by means of the pins strengthened by rotational springs. The Hamilton's principle is used during formulation of the boundary problem. The results of the numerical simulations are focused on the correction of the characteristic curves shape at a different radius of the loading head.

MSC 2010: *65Z05, 74H45, 74H55*
Keywords: *vibration, vibration control, stability, piezoceramic, characteristic curve*

1. Introduction

Mechanical structures are subjected to different static or dynamic excitations. The studies on the smart material lead to the point in which the integration of such materials with host structures took place to achieve the control over their behavior. One of those materials is a piezoceramic one. As a result of an applied voltage, the piezoceramic elements may generate additional forces which may lead to the bending [1] or prestressing [2]. This type of integration is possible because the piezoelements are being produced in a variety of shapes and sizes (rods, tubes, beams, discs, plates) and their mechanical properties.

In the studies [3], authors have presented the results on shape control of piezoelectric intelligent structures in the form of a structural plates. This paper included a mathematical model of a piezoelectric intelligent structure while the shape control was realized with the use of the genetic algorithm. Similar studies were realized in [4, 5]. Moreover, piezoelements can also be used when active dynamic instability control is a goal [6, 7].

In the paper written by Faria [8] one can find how to increase a buckling force of single beam with piezopart was presented. Author has used the system with both fixed ends, while the piezo has generated axial force. The studies performed by Sokół and Uzny [9] were focused on an influence of the residual longitudinal forces on the stability of the column subjected to Euler's load.

Sokół with cooperation with Przybylski [10] have eccentrically installed a piezoceramic rod in order to control the defection of the beam system. They have shown that application of a voltage to the piezoelement may help to regain the rectilinear form of static equilibrium.

The external load used in this study was defined by Tomski [11]. The loading unit generated the new shape of the characteristic curve known as the divergence - pseudoflutter one. The loading unit was composed of loading and load receiving heads with different parameters. That type of external load was called the specific one.

The main goal of this study is to perform theoretical and numerical studies on a cantilever multi-member column integrated with a piezorod. The studies are focused on an influence of the force generated by the piezoelement on the vibration frequency, shape of the characteristic curve as well as bifurcation load magnitude at a different radius of the loading head.

2. Investigated system

The investigated slender system is presented in Figure 1. The used loading heads have circular outlines.

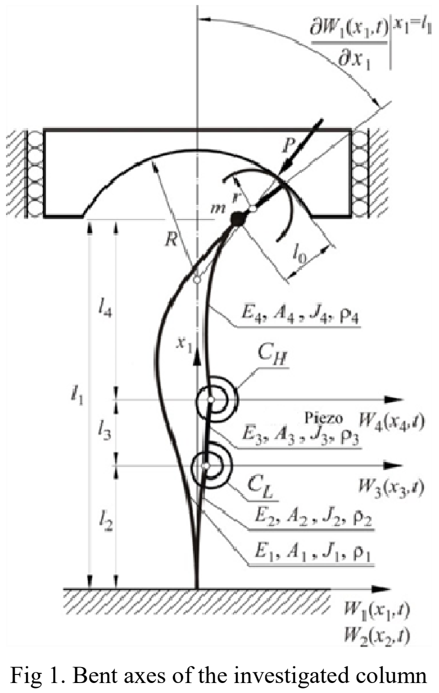

Fig 1. Bent axes of the investigated column

The system consists of two members - external and internal. The external one is composed of rod *1* which is a continuous element. The internal member is made of rods *2*, *3*, *4*. It is proposed that rod *3* will be made of piezoceramic material due to problematic production of long piezorods. The connection of the piezoelement with the internal elements *2* and *4* is realized with pins and rotational springs marked as C_L, C_H. Such a connection allows one to create a more general mathematical model on the basis of which studies on an influence of different parameters (associated with length and connection stiffness piezo - host structure) on vibration and stability can be done. The length of rods is marked with l_1, l_2, l_3, l_4 (where $l = l_1 = l_2 + l_3 + l_4$). The m stands for the mass of the heads while R is a radius of the loading head and r is a radius of the load receiving head. The l_0 describes the distance between the top end of the slender structure and the contact point of heads.

3. Problem formulation

In the first step of boundary problem formulation, the kinetic and potential energies were defined in the form:

$$T = \frac{1}{2}\sum_{i=1}^{4}\int_0^{l_i} \rho_i A_i \left[\frac{\partial W_i(x_i,t)}{\partial t}\right]^2 dx_i + \frac{1}{2} m \left[\left.\frac{\partial W_1(x_1,t)}{\partial t}\right|^{x_1=l_1}\right]^2 \tag{1}$$

$$\begin{aligned} V_1 = {} & \frac{1}{2}\sum_{i=1}^{4}\int_0^{l_i} E_i J_i \left[\frac{\partial^2 W_i(x_i,t)}{\partial x_i}\right]^2 dx_i + \frac{1}{2} C_L \left(\left.\frac{\partial W_3(x_3,t)}{\partial x_3}\right|_{x_3=0} - \left.\frac{\partial W_2(x_2,t)}{\partial x_2}\right|^{x_2=l_2}\right)^2 + \\ & + \frac{1}{2} C_H \left(\left.\frac{\partial W_4(x_4,t)}{\partial x_4}\right|_{x_4=0} - \left.\frac{\partial W_3(x_3,t)}{\partial x_3}\right|^{x_3=l_3}\right)^2 + \\ & + \frac{1}{2}\sum_{i=1}^{4} E_i A_i \int_0^{l_i}\left[\frac{\partial U_i(x_i,t)}{\partial x_i} + \frac{1}{2}\left(\frac{\partial W_i(x_i,t)}{\partial x_i}\right)^2\right]^2 \end{aligned} \tag{2a}$$

$$\begin{aligned} V_2 = {} & P U_1(l_1,t) - \frac{1}{2} P l_0 \left(\left.\frac{\partial W_1(x_1,t)}{\partial x_1}\right|^{x_1=l_1}\right)^2 + \\ & + \frac{1}{2} P r \left\{\left[\left.\frac{\partial W_1(x_1,t)}{\partial x_1}\right|^{x_1=l_1}\right]^2 - \chi^2\right\} + \frac{1}{2} P \chi W^* \end{aligned} \tag{2b}$$

where:

$$\chi = \frac{1}{R-r}\left(W_1(l_1,t) + (l_0 - r)\frac{\partial W_1(x_1,t)}{\partial x_1}\bigg|^{x_1=l_1} \right) \tag{3}$$

$$W^* = W_1(l_1,t) + \frac{\partial W_1(x_1,t)}{\partial x_1}\bigg|^{x_1=l_1}(l_0 - r) + r\chi \tag{4}$$

E_i - Young's modulus [GPa], J_i - moment of inertia [m^4], A_i - cross-sectional area [m^2], ρ_i - material density [kg/m^3], $C_{H,L}$ - rotational spring stiffness [Nm], P - external load [N], W_i - transversal displacement [m], U_i - longitudinal displacement [m], R - radius of the loading head [m], r - radius of the load receiving head [m], m - mass of heads [kg], l_0 - transom length [m].

The energies are substituted into the Hamilton's principle:

$$\delta\int_{t_1}^{t_2}\left[T - (V_1 + V_2)\right]dt = 0 \tag{5}$$

and after variation and integration operations, one may obtain equations of motion ($i = 1 \ldots 4$):

$$\begin{aligned} &E_i J_i \frac{\partial^4 W_i(x_i,t)}{\partial x_i^{\,4}} - E_i A_i \frac{\partial}{\partial x_i}\left[\left[\frac{\partial U_i(x_i,t)}{\partial x_i} + \frac{1}{2}\left(\frac{\partial W_i(x_i,t)}{\partial x_i}\right)^2\right]\frac{\partial W_i(x_i,t)}{\partial x_i}\right] + \\ &+ \rho_i A_i \frac{\partial^2 W_i(x_i,t)}{\partial t^2} = 0 \end{aligned} \tag{6}$$

and a set of natural boundary conditions which satisfy the continuity of displacements, longitudinal forces, deflection angles and bending moments. The natural boundary conditions are supplemented by the geometrical ones. The full set of boundary conditions is given below:

$$W_1(x_1,t)\big|_{x_1=0} = 0,\ \frac{\partial W_1(x_1,t)}{\partial x_1}\bigg|_{x_1=0} = 0,\ W_2(x_2,t)\big|_{x_2=0} = 0,\ \frac{\partial W_2(x_2,t)}{\partial x_2}\bigg|_{x_2=0} = 0 \tag{7-10}$$

$$W_2(x_2,t)\big|^{x_2=l_2} = W_3(x_3,t)\big|_{x_3=0},\ W_3(x_3,t)\big|^{x_3=l_3} = W_4(x_4,t)\big|_{x_4=0} \tag{11-12}$$

$$W_1(x_1,t)\big|^{x_1=l_1} = W_4(x_4,t)\big|^{x_4=l_4},\ \frac{\partial W_1(x_1,t)}{\partial x_1}\bigg|^{x_1=l_1} = \frac{\partial W_4(x_4,t)}{\partial x_4}\bigg|^{x_4=l_4} \tag{13-14}$$

$$-E_3 J_3 \frac{\partial^2 W_3(x_3,t)}{\partial x_3^2}\bigg|_{x_3=0} + C_L\left(\frac{\partial W_3(x_3,t)}{\partial x_3}\bigg|_{x_3=0} - \frac{\partial W_2(x_2,t)}{\partial x_2}\bigg|^{x_2=l_2}\right) = 0 \tag{15}$$

$$E_2 J_2 \left.\frac{\partial^2 W_2(x_2,t)}{\partial x_2^2}\right|^{x_2=l_2} - C_L \left(\left.\frac{\partial W_3(x_3,t)}{\partial x_3}\right|_{x_3=0} - \left.\frac{\partial W_2(x_2,t)}{\partial x_2}\right|^{x_2=l_2} \right) = 0 \tag{16}$$

$$-E_4 J_4 \left.\frac{\partial^2 W_4(x_4,t)}{\partial x_4^2}\right|_{x_4=0} + C_H \left(\left.\frac{\partial W_4(x_4,t)}{\partial x_4}\right|_{x_4=0} - \left.\frac{\partial W_3(x_3,t)}{\partial x_3}\right|^{x_3=l_3} \right) = 0 \tag{17}$$

$$E_3 J_3 \left.\frac{\partial^2 W_3(x_3,t)}{\partial x_3^2}\right|^{x_3=l_3} - C_H \left(\left.\frac{\partial W_4(x_4,t)}{\partial x_4}\right|_{x_4=0} - \left.\frac{\partial W_3(x_3,t)}{\partial x_3}\right|^{x_3=l_3} \right) = 0 \tag{18}$$

$$\begin{aligned} &E_2 J_2 \left.\frac{\partial^3 W_2(x_2,t)}{\partial x_2^3}\right|^{x_2=l_2} + S_2 \left.\frac{\partial W_2(x_2,t)}{\partial x_2}\right|^{x_2=l_2} + \\ &- E_3 J_3 \left.\frac{\partial^3 W_3(x_3,t)}{\partial x_3^3}\right|_{x_3=0} - S_3 \left.\frac{\partial W_3(x_3,t)}{\partial x_3}\right|_{x_3=0} = 0 \end{aligned} \tag{19}$$

$$\begin{aligned} &E_3 J_3 \left.\frac{\partial^3 W_3(x_3,t)}{\partial x_3^3}\right|^{x_3=l_3} + S_3 \left.\frac{\partial W_3(x_3,t)}{\partial x_3}\right|^{x_3=l_3} + \\ &- E_4 J_4 \left.\frac{\partial^3 W_4(x_4,t)}{\partial x_4^3}\right|_{x_4=0} - S_4 \left.\frac{\partial W_4(x_4,t)}{\partial x_4}\right|_{x_4=0} = 0 \end{aligned} \tag{20}$$

$$\begin{aligned} &E_1 J_1 \left.\frac{\partial^2 W_1(x_1,t)}{\partial x_1^2}\right|^{x_1=l_1} + E_4 J_4 \left.\frac{\partial^2 W_4(x_4,t)}{\partial x_4^2}\right|^{x_4=l_4} + \\ &+ P \frac{r-l_0}{R-r} \left(\left.\frac{\partial W_1(x_1,t)}{\partial x_1}\right|^{x_1=l_1} (R-l_0) - W_1(x_1,t)\Big|^{x_1=l_1} \right) = 0 \end{aligned} \tag{21}$$

$$S_1 + S_2 = P, \;\; S_2 = S_3 = S_4, \tag{22-24}$$

$$\begin{aligned} &E_1 J_1 \left.\frac{\partial^3 W_1(x_1,t)}{\partial x_1^3}\right|^{x_1=l_1} + E_4 J_4 \left.\frac{\partial^3 W_4(x_4,t)}{\partial x_4^3}\right|^{x_4=l_4} + \\ &+ P \frac{1}{R-r} \left(\left.\frac{\partial W_1(x_1,t)}{\partial x_1}\right|^{x_1=l_1} (R-l_0) - W_1(x_1,t)\Big|^{x_1=l_1} \right) - m \left.\frac{\partial^2 W_1(x_1,t)}{\partial t^2}\right|^{x_1=l_1} = 0 \end{aligned} \tag{25}$$

In order to designate the magnitude of the force generated by the piezoceramic element after the appliance of the voltage, one defines the potential energy in the form:

$$E_p = \frac{1}{2}\sum_{i=1}^{4}\int_{\Omega_i}\sigma_{xi}\varepsilon_{xi}d\Omega_i - \frac{1}{2}\int_{\Omega_p} D_z E_z d\Omega_p \tag{26}$$

The stress-strain relationships are given with eqs. (27)-(29). Electrical displacement induced by electrical field E_z is described by eq. (30). The other markings are as follows: ε_{xi} - axial strain, E_i - Young's modulus, e_{31} - piezoelectric constant, ψ_{33} - piezoelectric conductivity.

$$\sigma_{xi} = E_i\varepsilon_{xi}\left(x_i\right)\ i=1,2,4 \quad \varepsilon_{xi} = \frac{dU_i\left(x_i\right)}{dx_i}\ i=1,2,4 \tag{27, 28}$$

$$\sigma_{x3} = E_3\varepsilon_{x3}\left(x_3\right) - e_{31}E_z \quad D_z = e_{31}\varepsilon_{x3}\left(x_3\right) + \psi_{33}E_z \tag{29, 30}$$

The electric field and piezoelectric force one defines as $E_z = V/h$ and $F = -be_{31}V$ respectively.

Finally, after a series of mathematical operations (assuming that the voltage is constant), one obtains the formula which presents the relationship between parameters of the system and the piezoelectric force F. Such a force is called the residual one and is marked as F_{Rez}.

$$\begin{gathered} F_{\text{Rez}} = F\frac{E_1A_1E_2A_2E_4A_4l_3}{E_3A_3Ql_2 + E_2A_2\left(Ql_3 + E_3A_3\left(E_4A_4l_1 + E_1A_1l_4\right)\right)} \\ Q = E_1A_1E_4A_4 \end{gathered} \tag{31}$$

An induction of the residual force (by appliance of the voltage to the piezoceramic rod) lead to the prestressing of the system. One can find cases in which: the members are tensioned/compressed alternately (at low magnitude of external load) or the residual force balances the components of the forces in rods which appear during action of the external load. It should be also mentioned that the absolute value of F_{Rez} in rods is the same. Finally, the prestressing force must be introduced into (eq. (6)). The final solution of the boundary problem has been performed with the small parameter method [12].

4. Results

In this section the results of numerical simulations on an influence of the voltage applied to the piezorod on the shape of the bifurcation load curves and characteristic ones are presented. The results are plotted in the non-dimensional form, according to the following relations:

$$p=\frac{Pl^2}{E_1J_1+E_2J_2},\ f=\frac{Fl^2}{E_1J_1+E_2J_2},\ c_L=\frac{C_Ll}{E_1J_1+E_2J_2},\ c_H=\frac{C_Hl}{E_1J_1+E_2J_2},$$
$$r_{21}=\frac{E_2J_2}{E_1J_1},\ r_{32}=\frac{E_3J_3}{E_2J_2},\ r_{43}=\frac{E_4J_4}{E_3J_3},\ \zeta_A=\frac{R}{l_1},\ \zeta_B=\frac{r}{R},\ \zeta_C=\frac{l_0}{R}, \tag{32a-n}$$
$$\zeta_D=\frac{m}{(\rho_1A_1+\rho_2A_2)l},\ \omega=\sqrt{\Omega^2\frac{(\rho_1A_1+\rho_2A_2)l^4}{E_1J_1+E_2J_2}},\ d_2=\frac{l_2}{l},\ d_3=\frac{l_3}{l}$$

The results of the numerical simulations are plotted at a different magnitude of ζ_A = 0.2, 0.8, 1.6. The parameter represents the change in the radius of the loading head. The obtained curves are plotted on planes: external load magnitude p - prestressing force f and external load magnitude p vibration frequency ω. The other parameters of the system are given in the description below each figure. The $-f$ stands for tensile force in the external member.

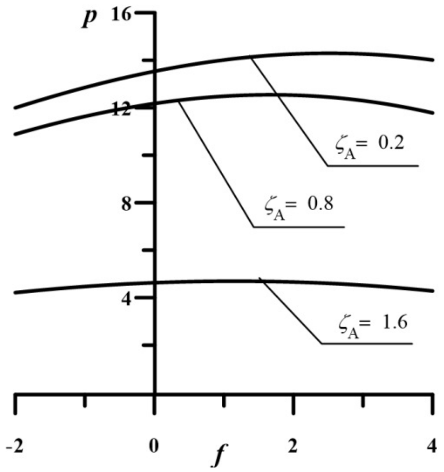

Fig. 2. Influence of the residual force f on bifurcation load p at different radius of the loading head (ζ_B = 0.2, ζ_C = 0.2, $r_{21} = r_{32} = r_{43}$ = 1, d_2 = 0.25, d_3 = 0.5, $c_H = c_L$ = 1)

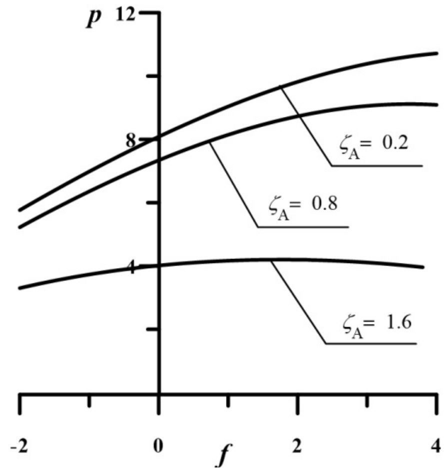

Fig. 3. Influence of the residual force f on bifurcation load p at different radius of the loading head (ζ_B = 0.2, ζ_C = 0.2, $r_{21} = r_{32} = r_{43}$ = 1, d_2 = 0.25, d_3 = 0.5, c_H = 0.1, c_L = 1)

When both rotational springs have equal stiffness ($c_H = c_L = 1$, see Fig. 2) the greatest increase in bifurcation load capacity has been observed at ζ_A = 0.2. An increase in ζ_A results in a decrease in the bifurcation load as well as an influence of the residual force becoming smaller. The reduction of the stiffness of one of springs down to c_H = 0.1 (Fig. 3) shows the analogues situation to the one described previously. It is worth mentioning that at the same magnitude of f more rapid changes in the bifurcation load (increase/decrease) can be observed in relation to the $c_H = 1$ case.

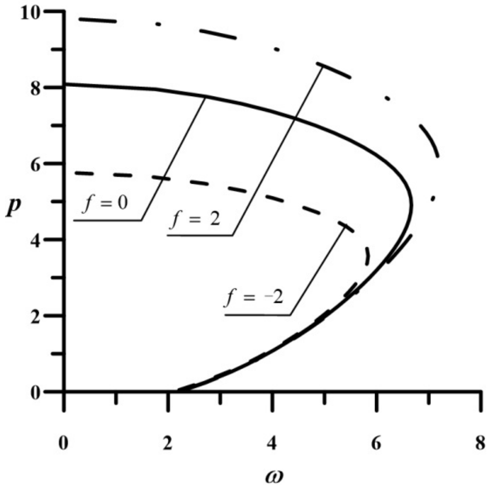

Fig. 4. Influence of the residual force f on the shape of the characteristic curves ($\zeta_A = 0.2$, $\zeta_B = 0.2$, $\zeta_C = 0.2$, $\zeta_D = 0.2$, $r_{21} = r_{32} = r_{43} = 1$, $d_2 = 0.25$, $d_3 = 0.5$, $c_H = 0.1$, $c_L = 1$)

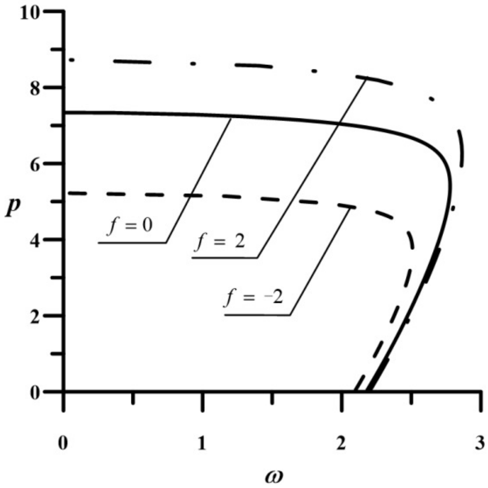

Fig. 5. Influence of the residual force f on the shape of the characteristic curves ($\zeta_A = 0.8$, $\zeta_B = 0.2$, $\zeta_C = 0.2$, $\zeta_D = 0.2$, $r_{21} = r_{32} = r_{43} = 1$, $d_2 = 0.25$, $d_3 = 0.5$, $c_H = 0.1$, $c_L = 1$)

On the basis of the data obtained during simultaneously performed studies one can present the characteristic curves on the external load - vibration frequency plane. The presented curves correspond to the case when $\zeta_B = 0.2$, $\zeta_C = 0.2$, $\zeta_D = 0.2$, $d_2 = 0.25$, $d_3 = 0.5$, $c_H = 0.1$, $c_L = 1$ and equal bending rigidity ratios. The ζ_A defines as 0.2 or 0.8. The curves are plotted at a different level of the prestressing force.

An appliance of a voltage to the piezoelement and generation of the tensile force in the external member ($-f$) results in reduction both in the vibration frequency as well as in the bifurcation load. The opposite results (increase in vibration frequency and bifurcation load) can be observed when the piezoforce causing the compression of the external member takes place ($+f$). Such a relation was observed at every considered magnitude of ζ_A. The change of the parameters of the heads such as ζ_B or ζ_C affects only the shape of the curves but not an influence of the prestressing.

An influence of the prestressing realized with the use of the piezoceramic elements on vibration modes is presented in Table 1.

The figures in Table 1 are presented at a different magnitude of the prestressing force as well as external load. Bearing in mind that the investigated system has a divergence-pseudoflutter type of the characteristic curve, one presents two vibration modes one for positive and one for negative slope of the curve.

Table 1. Influence of the prestressing on vibration modes ($\zeta_A = 0.2$, $\zeta_B = 0.2$, $\zeta_C = 0.2$, $\zeta_D = 0.2$, $r_{32} = r_{43} = 1$, $d_2 = 0.25$, $d_3 = 0.5$, $c_L = 1$, $c_H = 0.1$)

$f = 2$	
$p = 2$	$p = 9$
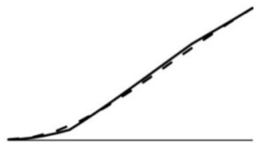	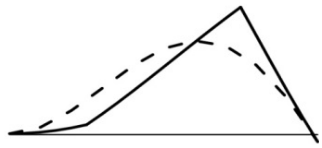
$f = 0$	
$p = 2$	$p = 7.8$
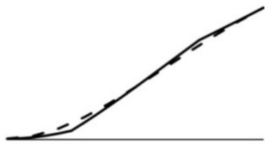	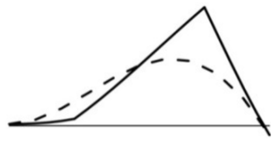
$f = -2$	
$p = 2$	$p = 5.5$
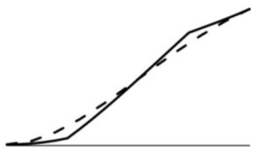	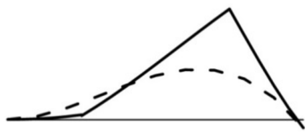

The continuous curve corresponds to the internal member while the continuous one stands for the external one. The generation of the presstressing equal to $f = 2$ results in shift of the bent axes of rods closer to each other when at $f = 0$ at greater p. At $f = -2$ the prestressing causes a greater deflection of axes of rods (at smaller p) in relation to the reference case ($f = 0$).

5. Conclusions

The paper presents the results of theoretical as well as numerical studies on a possibility of vibration and stability control by means of the piezoceramic elements at different loading heads used to generate the specific load. The piezoelement is connected to the main structure with the use of pins and rotational springs.

On the basis of the results of numerical simulations the general conclusions are:

- the compressive as well as tensile forces induced by the piezoelement allows one to observe vibration and bifurcation load control,
- an area of increase in bifurcation load depends not only on applied voltage but also on other parameters of the system for example spring stiffness,
- prestressing generated with piezoelement affects the shape and location of characteristic curves as well as the maximum vibration frequency magnitude.

As shown in this study, the piezorods can control the instability and vibrations of the slender systems. In future studies, an influence of the force generated by the piezoelement on the behavior of the main structure will be investigated taking into account the change in the load receiving head radius and transom length.

References

[1] Przybylski, J., & Kuliński, K. (2019). Shape enhancement of an eccentrically loaded column using piezoelectric actuator. *Engineering Structures*, *189*, 644-654.

[2] Przybylski, J., & Sokół, K. (2012). Chapter 10: The phenomenon of divergence and flutter instability control of a nonlinear system by means of a piezoelectric force. Free vibrations and stability of slender systems subjected to conservative and non-conservative loads (in Polish), Warszawa: WNT.

[3] Wang, Z., Qin, X., Zhang, S., Bai, J., Li, J., & Yu, G. (2017). *Optimal shape control of piezoelectric intelligent structure based on genetic algorithm, advances in materials science and engineering*. https://doi.org/10.1155/2017/6702183.

[4] Lin, J.C., & Nien, M.H. (2007). Adaptive modeling and shape control of laminated plates using piezoelectric actuators. *Journal of Materials Processing Technology*, *189*(1-3), 231-236.

[5] Agrawal, B.N., Elshafei, M.A., & Song G. (1997). Adaptive antenna shape control using piezoelectric actuators. *Acta Astronautica*, *40*(11), 821-826.

[6] Heganna, S., & Joglekar, J. (2016). Active vibration control of smart structure using PZT patches. *Procedia Computer Science*, *89*, 710-715.

[7] Sui, L., Xiong, X., & Shi, G. (2012). Piezoelectric actuator design and application on active vibration control. *Physics Procedia*, *25*, 1388-1396.

[8] Faria, A.R. (2004). On buckling enhancement of laminated beams with piezoelectric actuators via stress stiffening. *Composite Structures*, *65*(2), 187-192.

[9] Sokół, K., & Uzny S., (2015). Linear and nonlinear vibrations control of a two member column by means of piezoceramic element. AIP Conference Proceedings 1648. https://doi.org/10.1063/1.4913076.

[10] Przybylski, J., & Sokół K. (2011). Shape control of an eccentrically loaded column by means of a piezoceramic rod. *Thin - Walled Structures*, *49*, 652-659.

[11] Tomski, L., & Uzny, S. (2013). Vibrations and stability of a column subjected to the specific load realized by circular elements of heads. *Mechanics and Mechanical Engineering*, *17*, 197-206.

[12] Nayfeh, A.H. (1973). *Perturbation Methods*. New York: Wiley&Sons.